Prediction of polar ordered oxynitride perovskites

Razvan Caracas

Geophysical Laboratory, Carnegie Institution of Washington, 5251 Broad Branch Road, N.W., Washington DC 20015, USA and Bayerisches Geoinstitut, University of Bayreuth, Universitaetstrasse 30, D-95446 Bayreuth, Germany, e-mail: razvan.caracas@uni-bayreuth.de

R.E. Cohen

Geophysical Laboratory, Carnegie Institution of Washington, 5251 Broad Branch Road, N.W., Washington DC 20015, USA

(Dated: February 5, 2008)

Abstract

Using a *materials by design* approach, we find a class of ordered oxynitride piezoelectrics with perovskite structure. We predict that ordered $YSiO_2N$ and $YGeO_2N$ are characterized by large nonlinear optic responses and by some of the largest polarizations known to-date.

Most piezoelectrics (PZs) or polar dielectrics are oxides, and those commonly used are Pb-bearing compounds. PZs transform mechanical energy into electrical energy and vice versa, and serve many uses ranging from medical ultrasound and actuators to non-linear optic devices [1]. Materials for high temperature and/or high electric field applications are highly desirable, like Pb-free PZ materials as mandated by European law.

We have applied a synthetic solid state chemistry approach using ab initio density functional calculations [2, 3, 4, 5, 6, 7] to search for useful materials. Instead of an automated search of hundreds of compositions, we used a chemical approach similar to what would be done to experimentally search for materials. We built the oxynitride structures starting from the ideal cubic ABO_3 perovskite structure by replacing in each unit cell one oxygen atom by one nitrogen (Fig. 1). In this way we aim to drive a stronger polar distortion due to the strong covalent bonding expected between the octahedrally coordinated B-cation and N, as well as the higher nominal ionic charge of N^{3-} compared with O^{2-}. The resulting structures are ordered and polar with tetragonal symmetry, *P*4*mm* space group and five atoms per unit cell. In order to balance the -7 valence of O_2N we tried several combinations of trivalent and tetravalent cations on the respectively A and B sites: $YSiO_2N$, $YGeO_2N$, $InTiO_2N$, $GaTiO_2N$, $BiTiO_2N$, $YTiO_2N$, $BiZrO_2N$, YCO_2N, $YSnO_2N$ and $YZrO_2N$.

We used the local density approximation (LDA) of the density functional theory [8, 9] with a planewave basis and pseudopotentials in the ABINIT implementation [10]. We employed Troullier-Martins pseudopotentials [11] with a 40 Ha kinetic energy cut-off. We computed the dynamical and dielectric properties and the coupled response of the energy to the stresses and electric fields using density functional perturbation theory [12, 13, 14].

We relaxed the *P*4*mm* atomic positions and cell parameters at zero pressure for each of the above compositions and checked the insulating/metallic character computing the electron band structure and the corresponding density of states. We found that $InTiO_2N$ and $GaTiO_2N$ are metallic and all the other compounds are insulators. We checked the dynamical stability for each composition computing the phonon band dispersion and from all the combinations of cations listed above only $YSiO_2N$ and $YGeO_2N$ were dynamically stable.

The crystal structure of the *P*4*mm* modification of $YSiO_2N$ and $YGeO_2N$ is shown in Figure 1 and the relevant structural parameters are listed in Table I. All the atoms are displaced relative to their positions in the centrosymmetric structures. The corresponding

cation displacements are 0.76 Å for Y and 0.61 Å for Si in $YSiO_2N$ and 0.82 Å for Y and 0.77 Å for Ge in $YGeO_2N$. These large displacements enhance the polar character of the structures but also deepen the potential wells: 1.54 eV per unit cell in $YGeO_2N$ and 0.63 eV in $YSiO_2N$. Due to these large potential wells, the polar structures will probably not be switchable, thus these are not predicted to be ferroelectric without modification.

Oxynitrides are generally produced by low-temperature ammonization processes, which do not allow chemical ordering to occur. [15, 16, 17, 18]. We have tested different atomic configurations and found that the ordered P4*mm* structure is the lowest in energy, *e.g.* lower by at least 0.25 eV/O_2N group for $YSiO_2N$ than any other disordered configuration. We conclude that even if ordering in the oxynitrides is difficult [19], the previous experimental structures were disordered because of fabrication techniques. We suggest that the ordered materials should be producible by high temperature methods or by molecular beam epitaxy. Thus here we discuss ordered polar materials.

The phonon band dispersions for the two structures are shown in Figure 2. All the modes are stable, indicating dynamical stability and thermodynamical (meta)stability. The elastic constants also indicate mechanical stability (Table II). The heat of formation of the oxynitrides relative to a mixture of YN (fcc structure) and SiO_2 or GeO_2 (quartz structure) shows stability for the PZ phases (-0.387 eV/unit cell for $YSiO_2N$ and -0.309 for $YGeO_2N$). With these stability criteria the PZ structures of the two oxynitrides are at least thermodynamically metastable and their large negative heat of formation suggests that they should be easily synthesized.

Both materials are insulators with large LDA band gaps, 2.6 eV in $YGeO_2N$ and 4.4 eV in $YSiO_2N$. The computed dielectric tensors are ϵ^{∞}=[4.37 4.37 4.49] and ϵ^{0}=[13.44 13.44 9.71] for $YSiO_2N$ and ϵ^{∞}=[4.60 4.60 5.01] and ϵ^{0}=[16.10 16.10 9.80] for $YGeO_2N$. Because of symmetry, the Born effective charges, $Z^{\alpha *}_{ij} = 1/\Omega \ \delta P_i/\delta \tau^{\alpha}_j$, where Ω is the unit cell volume, P_i is the polarization along the direction i and τ^{α}_j is the displacement of atom α along direction j at zero electric field, are diagonal. Their values in the PZ structures are listed in Table III. The Born effective charges are only slightly enhanced due to the absence of the p-d hybridization characteristic to other oxide perovskites [20, 21].

We computed the spontaneous polarization using the modern theory of polarization [22, 23, 24]. The Berry's phase polarization is a lattice of values, with a lattice spacing of $2e\mathbf{R}/\Omega$, where e is the electron charge and $\mathbf{R}$ are the lattice vectors. Polarization differ-

ences, however, are unambiguous. Experiments measure polarization changes (usually via hysteresis loops) and absolute polarizations are not measurable using standard methods. For ferroelectrics with small polarizations comparison between theory and experiment is straightforward, but in materials with large polarizations the lattice of polarizations measured for a single polar structure cannot be unambiguously reduced to an experimentally meaningful value, called the *effective* polarization, without additional computations [25, 26]. For tetragonal symmetry, only the z-component of P is non-zero. We obtained the formal polarization along the polar axis z as $\mathrm{P}_{Berry} = 130(\pm \mathrm{n}308)\mu C/cm^2$ for $YSiO_2N$ and $103(\pm \mathrm{n}293)\mu C/cm^2$ for $YGeO_2N$, where the polarization lattice spacing is indicated in parentheses. In order to find the effective polarization, we computed its value using the Born effective charges, Z* (Table III) and the displacement vectors from the ideal perovskite structure, $\mathbf{u}$: $\Delta P = \sum \mathbf{Z}^* \mathbf{u}$. This gives effective polarizations P_Z=-163 μC/cm^2 for $YSiO_2N$ and P_Z=-171 μC/cm^2 for $YGeO_2N$. These values are not identical to the Berry's phase because of the linear approximation, but are very close. Using these values, we see that the effective P_{Berry} is -178 μC/cm^2 for $YSiO_2N$ and -190 μC/cm^2 for $YGeO_2N$ and these are our best estimates. The direction of polarization is from the B ion towards the closer N. Figure 3 shows the polarization lattices and comparison of the effective polarization and the Berry's phase values. The Born effective charges vary with distortion (Fig. 3c and d), the absolute values of the charges being slightly larger for the centrosymmetric phase than the ferroelectric phase.

These values of the polarization are amongst the highest ever reported so far in the literature. For comparison the spontaneous polarization is 71 μC/cm^2 in $LiNbO_3$, 50 in $LiTaO_3$,[27], 70 in $Pb(Mg,Nb)O_3$ [28] and >150 for polycrystalline thin films of $BiFeO_3$[29]. Other large polarization are those computed for pure $PbTiO_3$ (88)[30], $BiFeO_3$ (90-100)[25], $PbVO_3$ (150)[31].

We computed the piezoelectric constants tensors, $d_{ijk} = d\epsilon_{ij}/d\varepsilon_k$, where ϵ is the stress tensor and ε the electric field, using the linear response theory of elasticity [14, 32] and obtained d_{121}=-12.5 pC/N, d_{333}=-8.3 pC/N and d_{113}=0.4 p/N values for $YSiO_2N$ and d_{121}=-20.5 pC/N, d_{333}=-5.5 pC/N and d_{113}=-0.5 pC/N values for $YGeO_2N$. We also calculated the non-linear optical coefficients, $d_{ijk} = \chi^{(2)}_{ijk}/2$ where $\chi^{(2)}_{ijk} = 3E^{\varepsilon_i \varepsilon_j \varepsilon_k}/V$ is the third-order derivative of the energy with respect to electric fields, via linear response [33], and obtained d_{113}=2.03 pm/V and d_{333}=-5.5 pm/V in $YSiO_2N$ and d_{113}=2.63 pm/V and d_{333}=-4.51 pm/V in $YGeO_2N$. The highest value to-date is shown by AANP, an organic material

with d_{311}=d_{113}=80 [34]. In KH_2PO_4, a commonly used non-linear optical material, the non-linear optical coefficients are on the order of 0.4 pm/V and in ADP on the order of 0.8 pm/V [35]. The electro-optic coefficients, c_{ijk}, obtained from $\Delta(\epsilon^{-1})_{ij} = \sum_k (c_{ijk}\varepsilon_k)$ where $(\epsilon^{-1})_{ij}$ is the inverse of the dielectric tensor, have values of c_{133}=-1.43 pm/V, c_{333}=0.64 pm/V and c_{331}=-1.32 pm/V for $YSiO_2N$ and c_{133}=-0.84 pm/V, c_{333}=1.06 pm/V and c_{331}=-1.77 pm/V for $YGeO_2N$.

The high spontaneous polarizations, the non-linear optic coefficients, and the large stability of the piezoelectric structures make both $YSiO_2N$ and $YGeO_2N$ promising materials with broad possible applications as piezoelectrics and non-linear dielectrics. In addition, they may be useful as X-ray and neutron generators via accelerations of ions at their surfaces [36] due to their high polarizations.

Acknowledgments

Razvan Caracas acknowledges I. Grinberg for useful discussions. We acknowledge support from the U.S. Office of Naval Research.

[1] A. Arnau (Ed.), *Piezoelectric transducers and applications*, Springer Verlag, Heidelber (2004).

[2] A. Franceschetti and A. Zunger, Nature **402**, 60 (1999).

[3] S.C. Erwin and I. Zutic, Nat. Mater. **3**, 410 (2004).

[4] P. Baettig, C.F. Schelle, R. LeSar, U.V. Waghmare and N.A. Spaldin, Chem. Mater. **17**, 1376 (2005).

[5] S.V. Dudiy and A. Zunger, Phys. Rev. Lett. **97**, 046401, (2006).

[6] D.I. Bilc and D.J. Singh, Phys. Rev. Lett. **96**, 147602 (2006).

[7] K. Kang, Y.S. Meng, J. Breger, C.P. Grey and G. Ceder, Science **311**, 977 (2006).

[8] P. Hohenberg and W. Kohn, Phys. Rev. **136**, B864 (1964).

[9] W. Kohn and L.J. Sham, Phys. Rev. **140**, A1133 (1965).

[10] X. Gonze, J.-M. Beuken, R. Caracas, F. Detraux, M. Fuchs, G.-M. Rignanese, L. Sindic, M. Verstraete, G. Zerah, F. Jollet, M. Torrent, A. Roy, M. Mikami, Ph. Ghosez, J.-Y. Raty and D.C. Allan, Comput. Mater. Sci. **25** 478 (2002).

[11] N. Troullier and J.L. Martins, Phys. Rev. B **43**, 1993 (1991).

[12] S. Baroni, S. de Gironcoli, A. Dal Corso and P. Giannozzi, Rev. Mod. Phys. **73**, 515 (2001).

[13] X. Gonze, G.-M. Rignanese and R. Caracas, Z. Kristall. 220, 458 (2005).

[14] D.R. Hamman, K.M. Rabe and D. Vanderbilt, Phys. Rev. B **72**, 033102 (2005).

[15] S.J. Clarke, B.P. Guinot, C.W. Michie, M.J.C. Calmont and M.J. Rosseinsky, Chem. Mater. **14**, 288 (2002).

[16] Y.-I. Kim, P.M. Wodward, K.Z. Baba-Kishi and C.W. Tai, Chem. Mater. **16**, 1267 (2004).

[17] R. Marchand, Y. Laurent, J. Guyader, P. L'Haridon and P. Verdier, J. Eur. Ceram. Soc. **8**, 197 (1991).

[18] M.S. Hegde, Proc. Indian Acad. Sci. (Chem. Sci.) **113**, 445 (2001).

[19] B. Ravel, K.-I. Kim, P.M. Woodward and C.M. Fang, Phys. Rev. B **73**, 184121 (2006).

[20] R.E. Cohen, Nature **358**, 136 (1992).

[21] Posternak, M., R. Resta, and A. Baldereschi, Phys. Rev. B **50**, 8911 (1994).

[22] R. D. King-Smith and D. Vanderbilt, Phys. Rev. B **47**, 1651 (1993).

[23] D. Vanderbilt and R. D. King-Smith, Phys. Rev. B **48**, 4442 (1994).

[24] R. Resta, Rev. Mod. Phys **66**, 899 (1995).

[25] J. B. Neaton, C. Ederer, U.V. Waghmare, N.A. Spaldin, and K.M. Rabe, Phys. Rev. B **71**, 014113 (2005).

[26] R. Resta and D. Vanderbilt, in Physics of Ferroelectrics: a Modern Perspective, Eds. C.H. Ahn, K.M. Rabe, and J.M. Triscone, Springer-Verlag, New York (2007).

[27] M.E. Lines and A. M. Glass, *Principles and applications of ferroelectrics and related materials*, Oxford Classics, Oxford University Press, Oxford (2001).

[28] Z. Kutnjak, J. Petzelt and R. Blinc, Nature **441**, 956 (2006).

[29] K.Y. Yun, D. Ricinschi, T. Kanashima, M. Noda and M. Okuyama, Japan. J. Appl. Phys. **43**, L647 (2004).

[30] G. Saghi-Szabo, R.E. Cohen and H. Krakauer, Phys. Rev. Lett. **80**, 4321 (1998).

[31] U. Yoshitaka, S. Tatsuya, I. Fumiyuki and O. Tamio, Jpn. J. Appl. Phys. **44**, 7130 (2005).

[32] Z. Wu and R.E. Cohen, Phys. Rev. Lett. **95**, 037601 (2005).

[33] M. Veithen, X. Gonze and Ph. Ghosez, Phys. Rev. B **71**, 125107 (2005).

[34] S. Tomaru, S. Matsumoto, T. Kurihara, H. Suzuki, N. Ooba and T. Kaino, Appl. Phys. Lett. **58**, 2583 (1991).

[35] R.C. Eckardt, R.L. Byer, H. Masuda and Y.X. Fan., IEEE J.Q. Electr. **26**, 922 (1990).

[36] B. Naranjo, J.K. Gimzewski and S. Putterman, Nature **4343**, 1115, (2005).

TABLE I: Structural parameters for $YSiO_2N$ and $YGeO_2N$ in the P4mm ferroic structures. Y, Ge/Si, O and N atoms are in 1b(1/2 1/2 z), 1a(0 0 z), 2c(1/2 0 z) and 1a Wyckhoff positions respectively.

	a(Å)	c(Å)	z_Y	$z_{Ge/Si}$	z_O	z_N
$YSiO_2N$	3.228	4.435	0.342	0.889	0.027	0.513
$YGeO_2N$	3.307	4.66	0.325	0.874	0.038	0.500

TABLE II: Elastic constants (in GPa) at zero pressure computed from density functional perturbation theory [12, 14].

	C_{11}	C_{33}	C_{12}	C_{13}	C_{44}	C_{66}
$YSiO_2N$	466	317	211	100	135	231
$YGeO_2N$	374	345	176	86	90	167

TABLE III: Born effective charge tensors, Z^*_{ij} in the ferroelectric phases of $YGeO_2N$ (columns 1-4) and $YSiO_2N$ (columns 5-8). Due to symmetry the tensors are diagonal.

Elem.	Z^*_{11}	Z^*_{22}	Z^*_{33}	Elem.	Z^*_{11}	Z^*_{22}	Z^*_{33}
Y	3.48	3.48	3.38	Y	3.47	3.47	3.22
Ge	3.58	3.58	3.84	Si	3.49	3.49	3.99
O	-2.74	-1.91	-2.34	O	-2.66	-1.84	-2.22
N	-2.40	-2.40	-2.54	N	-2.47	-2.47	-2.75

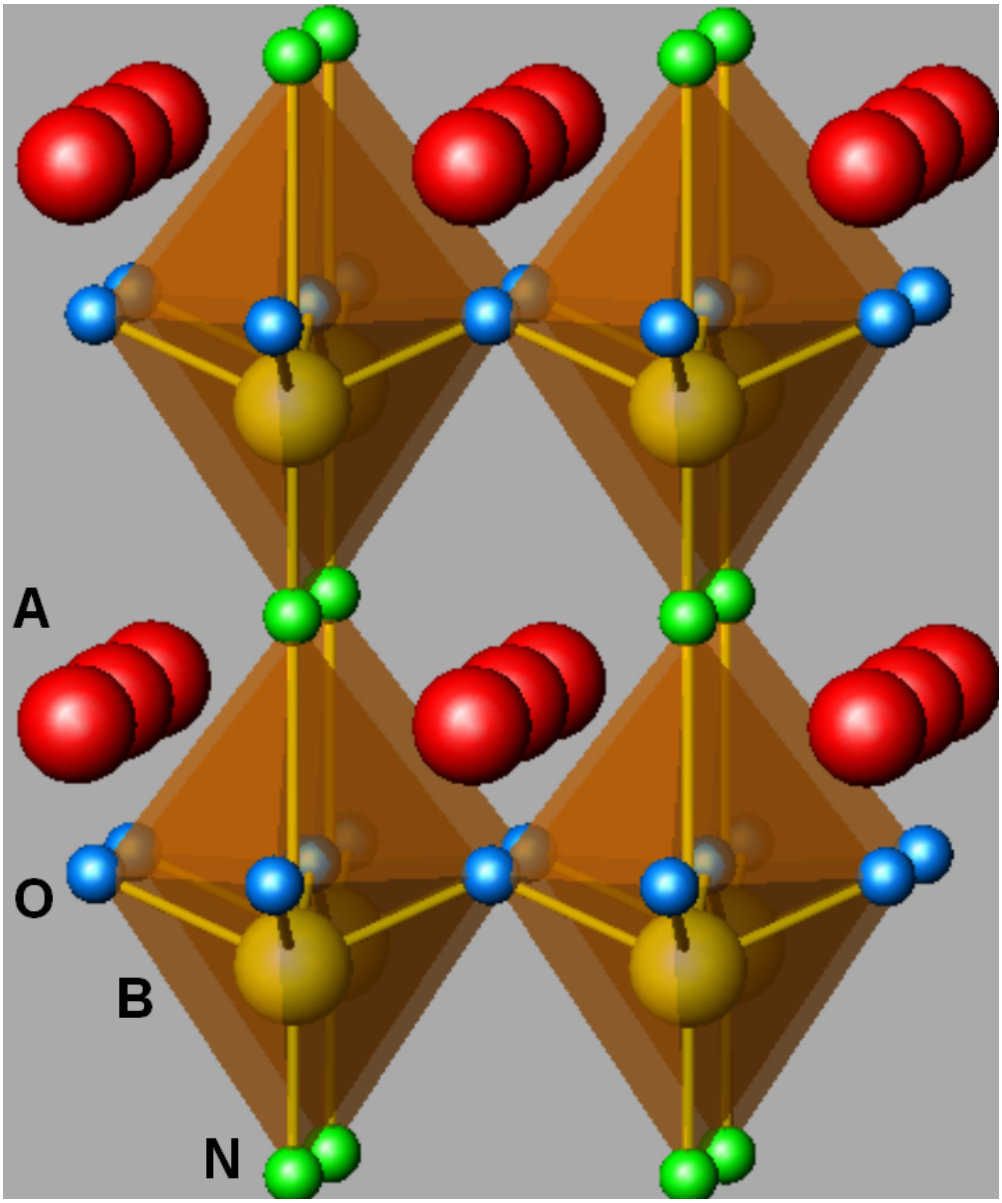

FIG. 1: Theoretical P4mm polar structure of the ordered ABO_2N oxynitride perovskites. The most promising materials we found have Y in the A site, and Si or Ge in the B site.

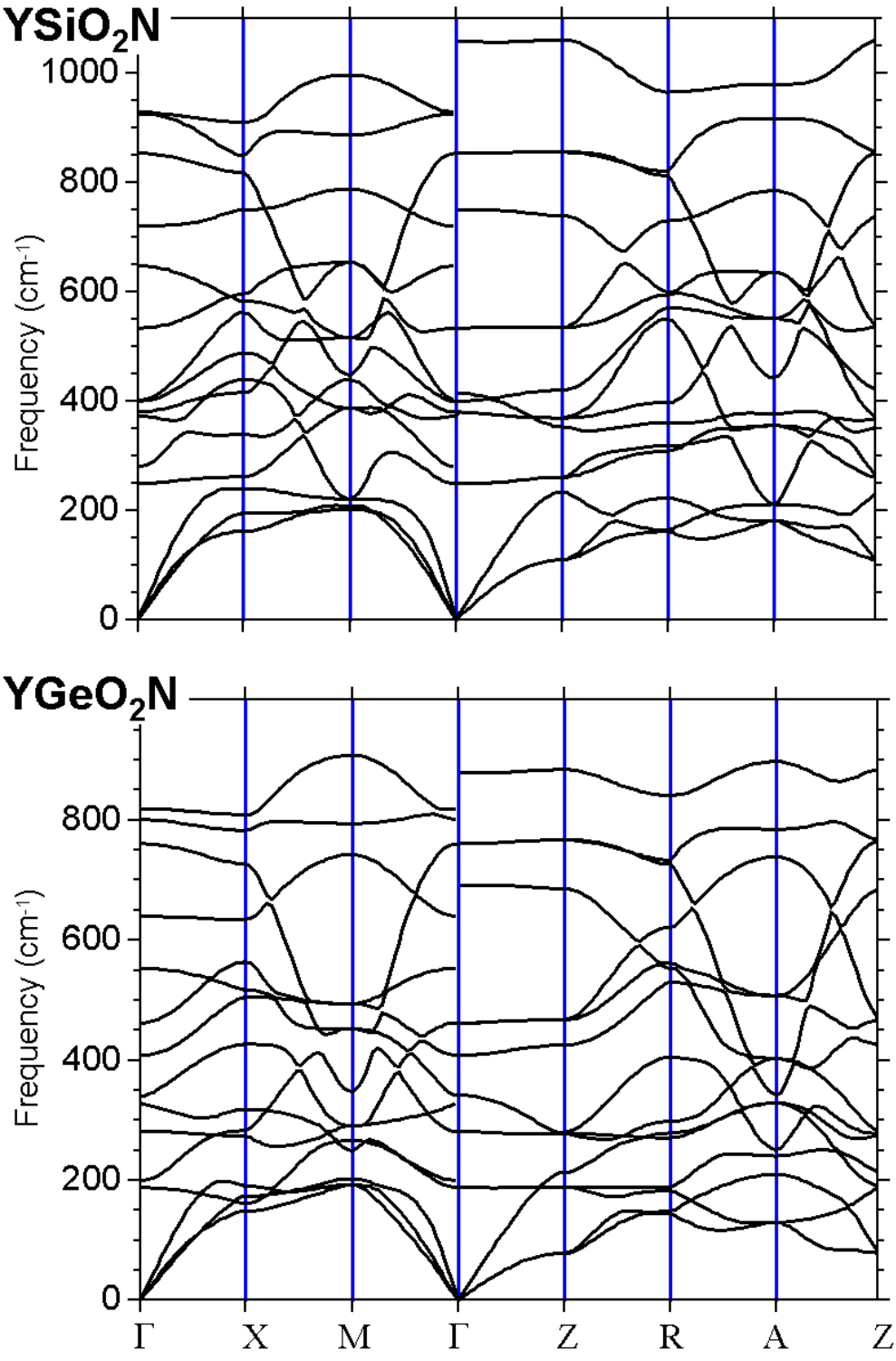

FIG. 2: Phonon band structure computed in the density functional perturbation theory for $YSiO_2N$ (a) and $YGeO_2N$ (b). The path through the Brillouin zone passes through: Γ=(0 0 0), X=(1/2 0 0), M=(1/2 1/2 0), Z=(0 0 1/2), R=(1/2 0 1/2), A=(1/2 1/2 1/2).

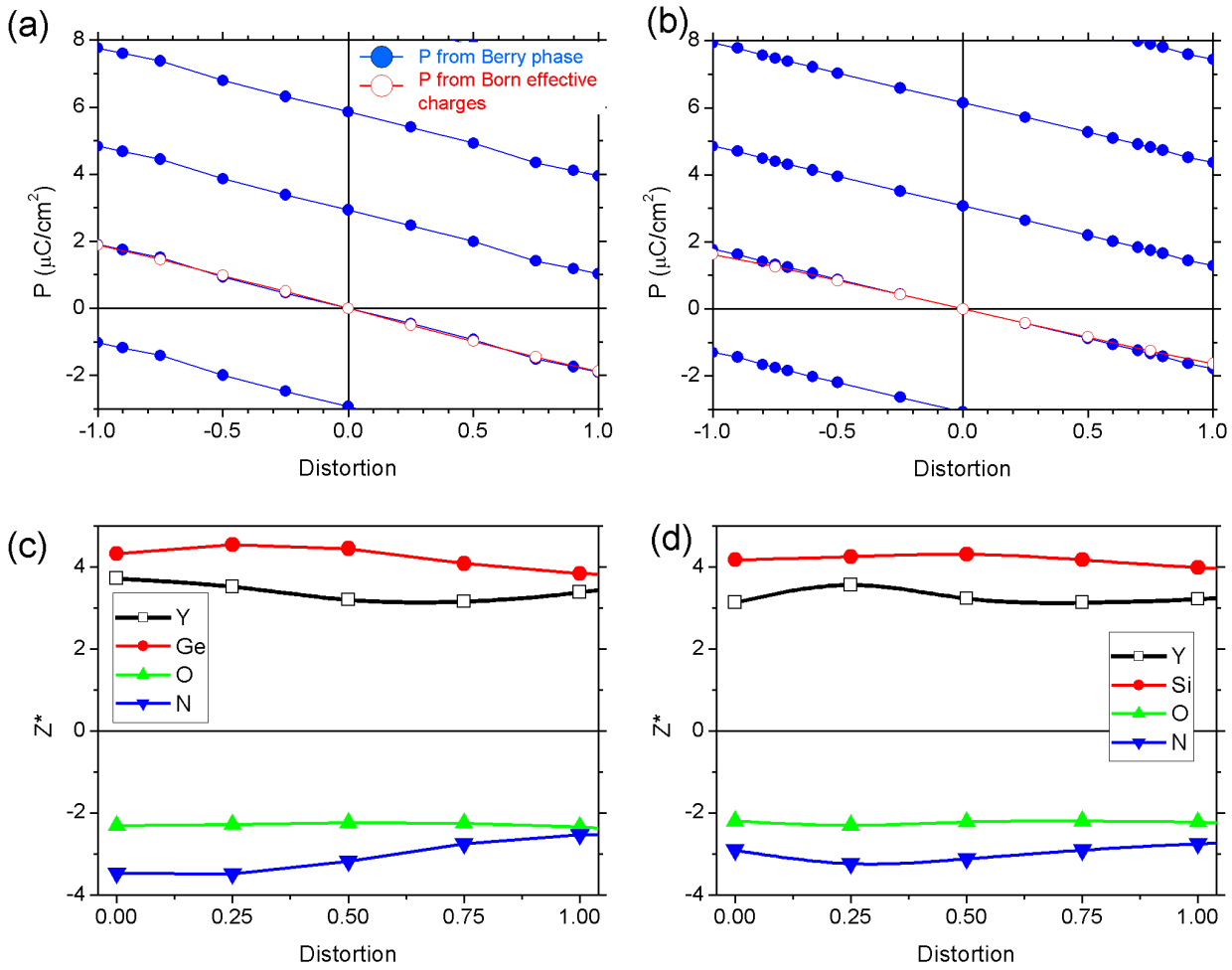

FIG. 3: The lattice of polarizations for $YGeO_2N$ (a) and $YSiO_2N$ (b) and the Born effective charges for $YGeO_2N$ (c) and $YSiO_2N$ (d) as a function of the position (=distortion) along the centrosymmetric-to-ferroelectric direct path.